

行政院國家科學委員會補助專題研究計畫 成果報告
 期中進度報告

堅硬土層侵入回填土對擋土牆靜止土壓力及主動土壓力之影響(3/3)

計畫類別： 個別型計畫 整合型計畫

計畫編號：NSC 96-2221-E-009-004-

執行期間：96年8月1日至97年7月31日

計畫主持人：方永壽教授

計畫參與人員：鄭詠誠、吳俊德 碩士班研究生

成果報告類型(依經費核定清單規定繳交)： 精簡報告 完整報告

本成果報告包括以下應繳交之附件：

- 赴國外出差或研習心得報告一份
- 赴大陸地區出差或研習心得報告一份
- 出席國際學術會議心得報告及發表之論文各一份
- 國際合作研究計畫國外研究報告書一份

處理方式：除產學合作研究計畫、提升產業技術及人才培育研究計畫、
列管計畫及下列情形者外，得立即公開查詢

涉及專利或其他智慧財產權， 一年 二年後可公開查詢

執行單位：國立交通大學土木工程學系

中華民國 97 年 7 月 31 日

堅硬土層侵入回填土對擋土牆靜止土壓力及主動土壓力之影響(3/3)

摘要

本研究探討堅硬土層侵入回填土對擋土牆主動土壓力之影響。本研究以氣乾之渥太華砂作為回填土，回填土高 0.5 公尺。量測於鬆砂($D_r = 35\%$)狀態下作用於剛性榜土牆的側向土壓力。本研究利用國立交通大學模型擋土牆設備來探討堅硬以不同界面傾角 β 侵入回填土對擋土牆主動土壓力影響。為了模擬堅硬的土層界面，本研究設計並建造一片鋼製傾斜界面板，及其支撐系統。本研究共執行五種堅硬界面傾角 $\beta = 0^\circ$ 、 50° 、 60° 、 70° 與 80° 五種實驗。依擋土牆砂實驗結果，本研究獲得以下幾項結論。(1) 當岩石界面傾角 $\beta = 0^\circ$ 時，其主動土壓力係數 $K_{a,h}$ 與 Coulomb 解相吻合，其主動合力約作用於距擋土牆底部 $0.33H$ 處。(2) 在岩石界面傾角為 45° 、 60° 、 70° 與 80° 狀況下，側向土壓力隨深度的增加而呈非線性分布，實驗所獲得的主動土壓力低於 Coulomb 解，主動土壓力隨界面傾角的增加而減少。(3) 當界面傾角為 50° 至 80° ，主動土壓力係數 $K_{a,h}$ 數隨岩石界面傾角的增加而逐漸減小。其合力作用點的位置會稍高於理論值 $0.333H$ 。(4) 當傾斜岩石面侵入主動土楔時，造成擋土牆抗滑動之安全係數增加，因此根據 Coulomb 理論所求解之安全係數會偏向安全。(5) 當傾斜岩石面侵入土楔時，使得擋土牆抗傾覆之安全係數增加，所以依據 Coulomb 理論所求得之安全係數會趨於安全。

關鍵詞：擋土牆;主動土壓力;回填土; 土壓力

Earth Pressure on Retaining Walls with Intrusion of a Stiff Interface into Backfill (3/3)

Abstract

This report studied the active earth pressure on retaining walls with the intrusion of an inclined rock face into the backfill. The instrumented model retaining-wall facilities at National Chiao Tung University was used to investigate the active earth pressure induced by different interface inclination angles. Loose Ottawa silica sand was used as the backfill material. To simulate an inclined rock face, a steel interface plate and its supporting system were designed and constructed. Base on the test results, the following conclusions can be drawn. (1) Without the Stiff interface ($\beta = 0^\circ$), the active earth pressure coefficient $K_{a,h}$ was in good agreement with Coulomb's equation. The point of application h/H of the active soil thrust was located at about $0.33H$ above the base of the wall. (2) For the interface inclination angle $\beta = 50^\circ, 60^\circ, 70^\circ$ and 80° , the distributions of active earth pressure were not linear with depth. On the lower part of the model wall the measured horizontal pressure was lower than Coulomb's prediction. (3) For $\beta = 50^\circ \sim 80^\circ$, the active earth pressure coefficient $K_{a,h}$ decreased with increasing interface inclination angle. The point of application of the active soil thrust moved a location slightly higher than $h/H = 0.333$. (4) For $\beta = 50^\circ \sim 80^\circ$, the nearby inclined rock face would actually increase the FS against sliding of the wall. The evaluation of FS against sliding with Coulomb's theory would be on the safe side. (5) For $\beta = 50^\circ \sim 80^\circ$, the intrusion of an inclined rock face into the active soil wedge would increase the FS against overturning of the retaining wall. The evaluation of FS against overturning with Coulomb's theory would also be on the safe side.

Keywords: Retaining wall; Active earth pressure; Backfill, Earth pressure

1. INTRODUCTION

In this study, the effects of an adjacent inclined rock face on the active earth pressure against a rigid retaining wall was studied. In tradition, active earth pressure behind a gravity-type retaining wall is estimated with either Coulomb's or Rankine's theory. However, if the retaining wall is constructed on the side of for a mountainside highway, adjacent to an inclined rock face as shown in Fig. 1.1, the nearby rock face might intrude the active soil wedge behind the wall. The distribution of earth pressure on the retaining wall might be affected by the presence of the inclined rock face. In the design of retaining walls in mountainous area, it is important to estimate the magnitude of the active soil thrust and the point of application of the active soil thrust. For gravity-type retaining walls, the Rankine's active failure wedge in the backfill is bounded by the wall and the plane with an inclination angle of $(45^\circ + \phi/2)$ from the horizontal, as shown in Fig. 1.1 The nearby rock face may interfere the development of the Rankine's active failure wedge behind the wall. For retaining walls built adjacent to stiff interface, can Coulomb's or Rankine's theory be used to evaluate the active earth pressure active on the wall? Would the distribution of active earth pressure still be linear with depth? The distribution of active earth pressure on retaining structures adjacent to an inclined stiff interface is discussed in this report.

1.1 Objective of Study

The NCTU model retaining wall facility was modified to study the effects of an adjacent inclined rock face on active earth pressure. A steel interface plate simulating the rock face was designed and constructed. A top supporting beam, and a base supporting block were constructed to support the steel interface plate. Air-dry Ottawa sand was used as the backfill material. For a loose backfill, the soil was placed behind the wall with the air-pluviation method to achieve a relative density of 35%. The main parameter considered for this study is the rock face inclination angle $\beta = 0^\circ, 50^\circ, 60^\circ, 70^\circ$, and 80° as shown in Fig. 1.2. The height of the backfill $H = 0.5$ m. The variation of lateral earth pressure was measured with the soil pressure transducers on the surface of the model wall. Based on experimental results, the distribution of earth pressure on the retaining wall adjacent an inclined interface was investigated. The test results would provide valuable information for geotechnical engineers regarding the design of retaining structures near an inclined rock face.

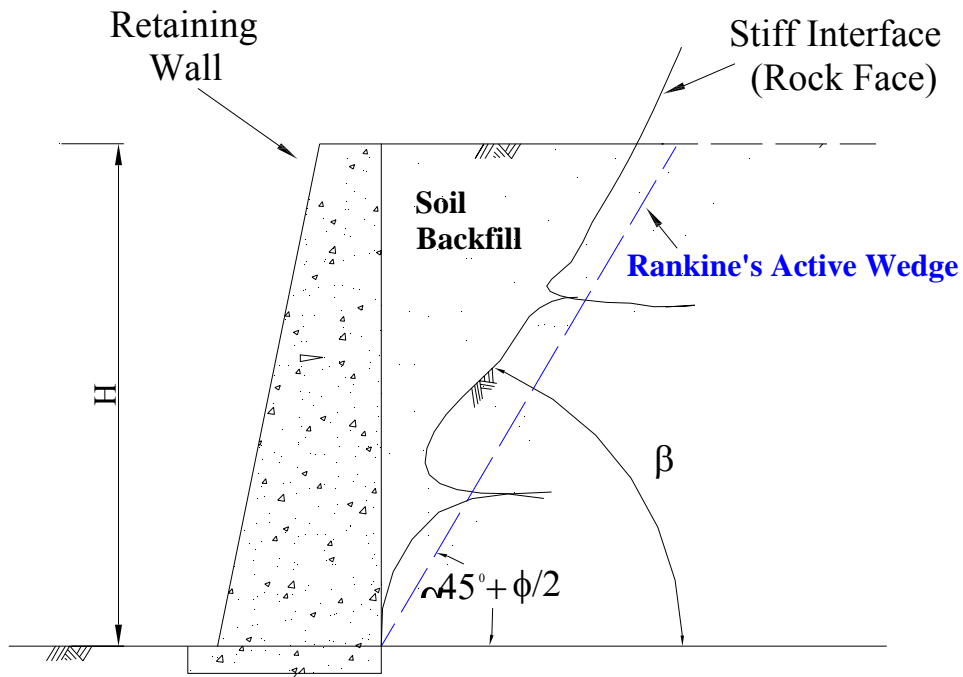


Fig. 1.1. Retaining walls with intrusion of a stiff interface into backfill

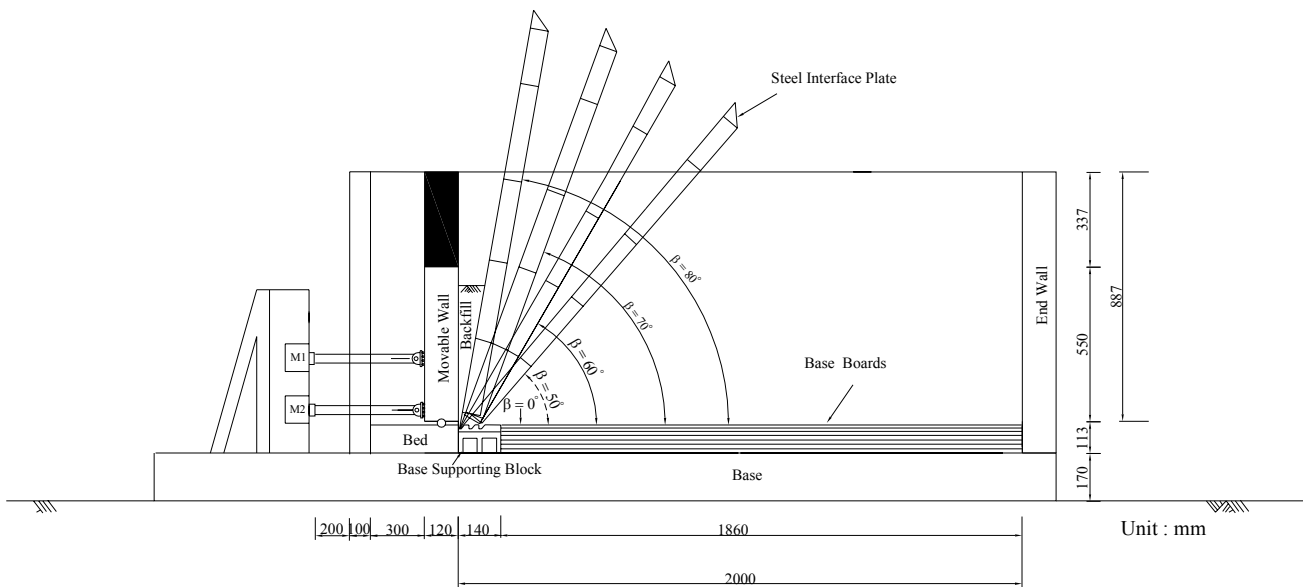


Fig. 1.2. Different interface inclinations

2. LITERATURE REVIEW

Geotechnical engineers frequently utilize the Coulomb and Rankine earth pressure theories to calculate the active earth pressure behind retaining structures. Terzaghi (1934), Mackey and Kirk (1967), Bros (1972), Sherif et al. (1982), Fang and Ishibashi (1986), Fang et al.(1994) and Fang et al.(1997) made experimental investigations regarding active earth pressure. Numerical investigation was studied by Bakeer and Bhatia (1989), Fang et al. (1993) and Matsuzawa and Hazarika (1996). Frydman and Keissar (1987) used the centrifuge technique to test a small mode. The change of pressure from the at-rest to the active condition for a retaining wall near a vertical rock face was observed. Fan and Chen (2006) used the non-linear finite element program PLAXIS to investigate the at-rest to the active condition for a rigid wall close to a stable rock face.

3. EXPERIMENTAL APPARATUS

In order to study the earth pressure behind retaining structures, the National Chiao Tung University (NCTU) has built a model retaining wall system which can simulate different kinds of wall movement. The entire system consists of the following components: (1) soil bin; (2) model retaining wall; (3) driving system; and (4) data acquisition system.

3.1 Soil Bin

The soil bin is 2,000 mm in length, 1,000 mm in width and 1,000 mm in depth as shown in Fig. 3.1. Both side walls of the soil bin are made of 30 mm thick transparent acrylic plates, through which the behavior of the backfill can be observed. The end wall that sits opposite to the model retaining wall is made of 100 mm-thick steel plates. The bottom of the soil bin is covered with a layer of Safety-Walk to provide adequate friction between the soil and the base of the soil bin.

To eliminate the friction between backfill and sidewall, a lubrication layer with 3 layers of plastic sheets was furnished for all model wall experiments. The lubrication layer consisted of one thick and two thin plastic sheets were hung vertically on each sidewall of the soil bin before the backfill was deposited. The thick sheet was placed next to the soil particles. It was expected that the thick sheet would help to smooth out the rough interface as a result of plastic-sheet penetration under normal stress. Two thin sheets were placed next to the steel sidewall to provide possible sliding planes.

3.2 Model Wall

The moveable retaining wall and its driving systems are shown in Fig. 3.1. The retaining wall is 1000 mm-wide, 550 mm-high, and 120 mm-thick, and is made of solid steel. The retaining wall is

vertically supported by two unidirectional rollers, and laterally supported by the steel frame through the driving system. Two separately controlled wall driving mechanisms, one at the upper level, and the other at the lower level, provide various kinds of lateral wall movements.

To investigate the earth pressure distribution, 9 earth pressure transducers were attached to the model wall as illustrated in Fig. 3.2. The soil pressure transducers were strain-gage-type transducers (PGM-02KG, capacity = 19.62kN/m²). To eliminate the soil arching effect, all soil pressure transducers were built quite stiff, and their measuring surfaces were flush with the face of the wall.

3.3 driving system

To achieve different modes of wall movement, two sets of driving rods were attached to the model wall. The upper driving rods were located 230 mm below the top of the wall, and the lower rods were located 236 mm below the upper rods as shown in Fig. 3.3. Two driving motors (ELECTRO, M-4621AB) supplied the thrust to the upper and the lower driving rods independently. The wall speed and movement modes were controlled by the automatic motor speed control system (DIGILOK, DLC-300) shown in Fig. 3.4. By setting the same motor speed for the upper and lower driving rods, a translational mode can be achieved for the model wall.

3.4 Data Acquisition System

The Data acquisition system used for this study composed of the following four parts: (1) dynamic strain amplifiers (Kyowa: DPM601A and DPM711B); (2) NI card; (3) AD/DA card; and (4) PC. The analog signals obtained from the sensors were filtered and amplified by dynamic strain amplifiers. Analog Experimental data were converted to digital data by the A/D - D/A card. The LabVIEW program was used to acquire experimental data. Experimental data were stored and analyzed with the Pentium 4 personal computer.

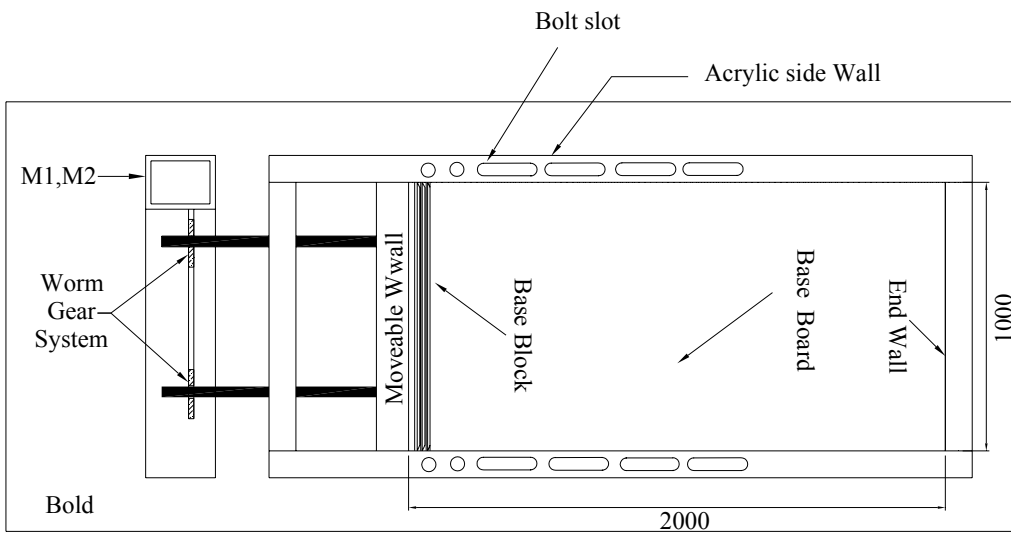
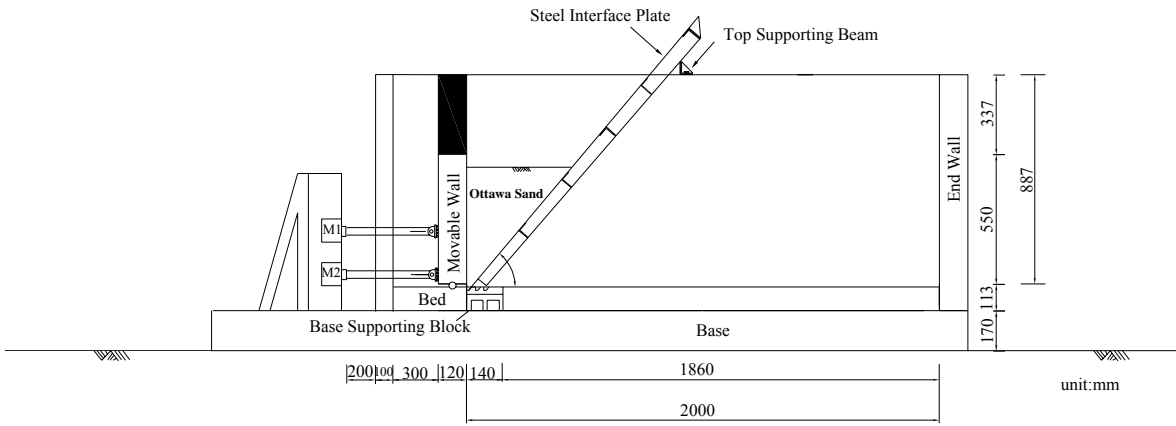


Fig.3.1. NCTU model retaining wall

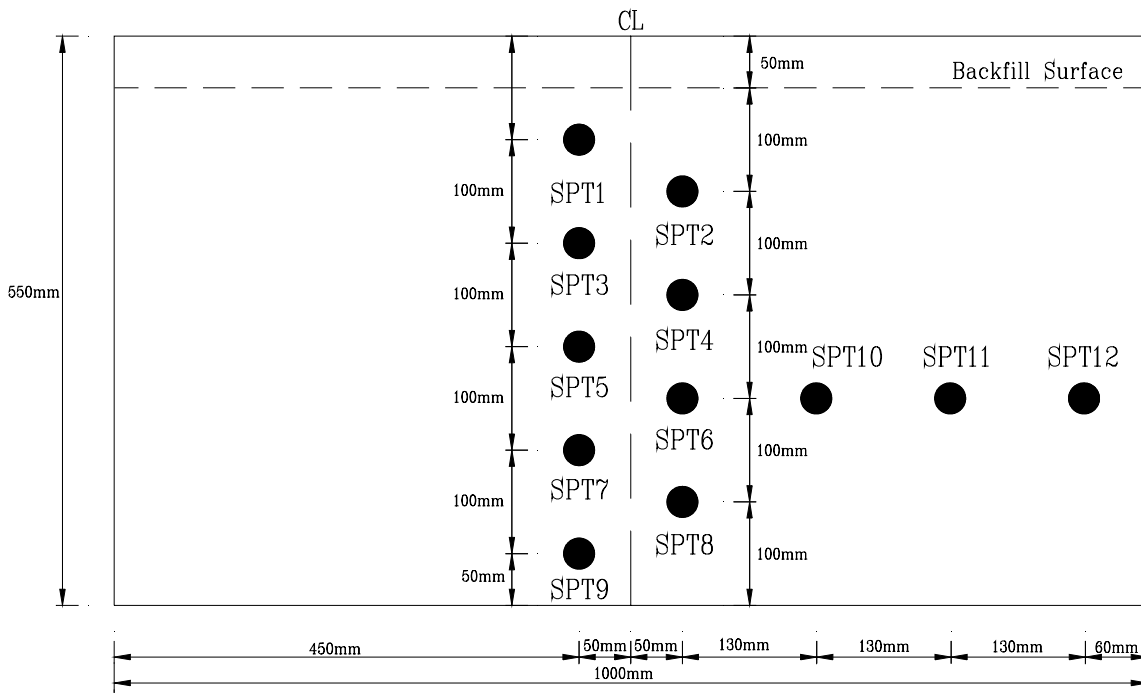


Fig.3.2. Location of pressure transducers on model wall

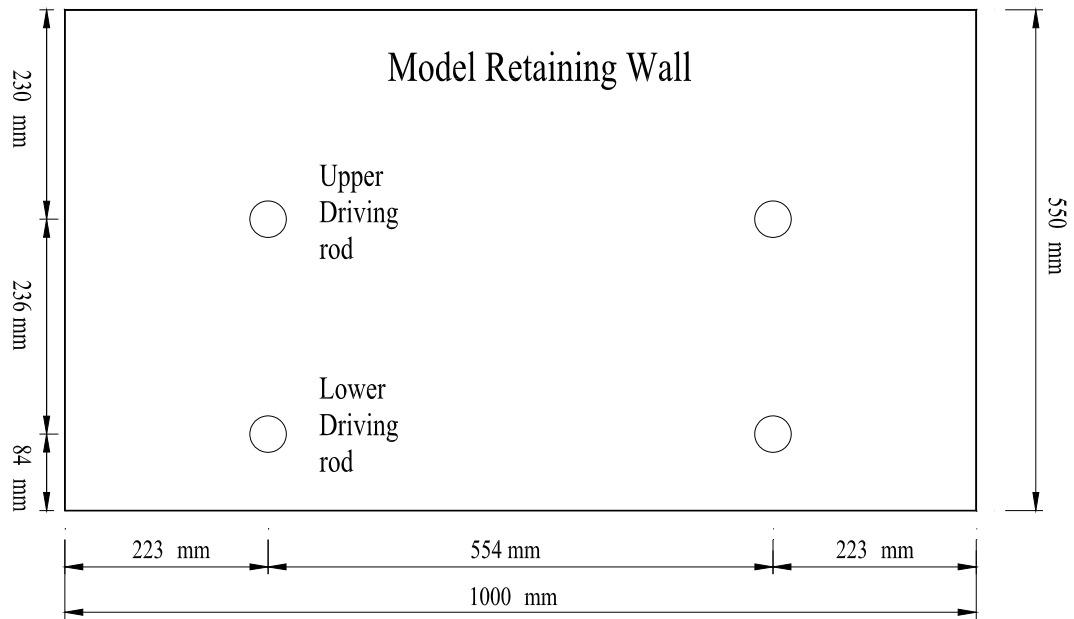


Fig.3.3. Location of driving rods

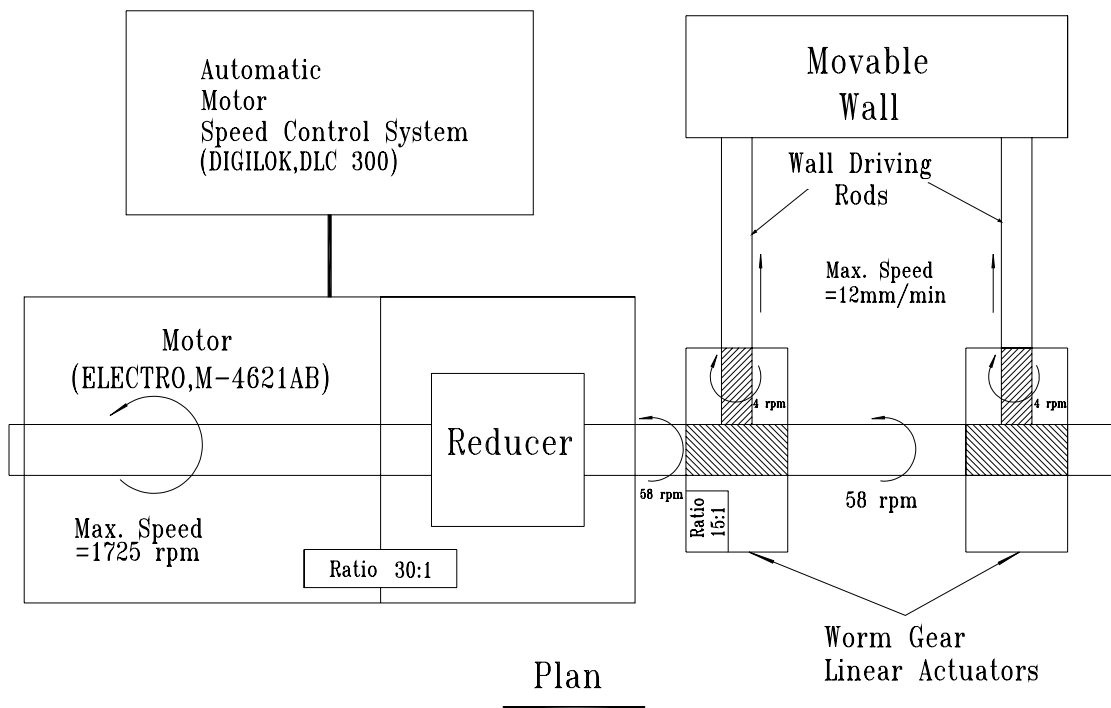


Fig.3.4. Wall speed control system

4. VERTICAL INTERFACE PLATE AND SUPPORTING SYSTEM

A steel interface plate was designed and constructed to simulate the inclined rock face near the retaining structure as shown in Fig. 1.1. In Fig. 4.1, the plate and its supporting system were developed to fit in the NCTU model retaining-wall facility. The system consists of the following two parts: (1) steel interface plate; and (2) supporting system. Details of the interface plate and its supporting system are introduced in the following sections.

4.1 Steel Interface Plate

The steel plate is 1.370 m-long, 0.998 m-wide, and 5 mm-thick as shown in Fig. 4.2. The unit weight of the steel plate is 76.52 kN/m^3 and its total mass is 53.32 kg (0.523 kN). A layer of anti-slip material (Safety-walk, 3M) was attached on the steel plate to simulate the friction that would act between the backfill and rock face as illustrated in Fig. 4.2 (c). A matrix of steel L-beams ($30 \text{ mm} \times 30 \text{ mm} \times 3 \text{ mm}$) were chosen as the reinforced material for the plate. On top of the interface plate, a $65 \text{ mm} \times 65 \text{ mm} \times 8 \text{ mm}$ steel L-beam was welded to reinforce the connection between the plate and the hoist ring shown in Fig. 4.2 (b).

4.2 Supporting System

To keep the steel interface plate in the soil bin stable during testing, a new supporting system for the interface plate was designed and constructed. The supporting system composed of the following two parts: (1) top supporting beam; and (2) base supporting block.

4.2.1 Top Supporting Beam

The top supporting steel beam was placed at the back of the interface plate and fixed at the bolt slot on the side walls of the soil bin. Details of top supporting beam were illustrated in Fig. 4.3. The section of supporting steel beam was $65 \text{ mm} \times 65 \text{ mm} \times 8 \text{ mm}$ and its length was 1700 mm. Fig. 4.4 showed the top supporting beam was fixed at the slots with bolts.

4.2.2 Base Supporting Block

The base block used to support the steel interface plate was shown in Fig. 4.5. The supporting block is 1.0 m-long, 0.14 m-wide, and 0.113 m-thick. Fig. 4.5 (b) showed three trapezoid grooves were carved on the face of the base supporting block. Fig. 4.6 showed the foot of the interface plate could be inserted into the groove at different distance from the model wall. Different horizontal spacing d adopted for testing included: (1) $d = 0 \text{ mm}$; (2) $d = 50 \text{ mm}$ and (3) $d = 100 \text{ mm}$. Fig. 4.6 showed 6 pieces of plywood boards were inserted between the base supporting block and the end wall to keep the base block stable. Details of base board were illustrated in Fig.

4.7. The base board was 1860 mm-long, 1002 mm-wide and 113 mm-thick. The surface of the top base board was cover with a layer of anti-slip material Safe-Walk.

4.3 Different Interface Inclinations

Different interface inclinations angles $\beta = 0^\circ, 50^\circ, 60^\circ, 70^\circ$ and 80° associated with this investigation were shown in Fig. 1.2. Fig. 4.8 showed the arrangement of model wall, plastic sheets interface plate and Ottawa sand test conditions for the interface inclination angle $\beta = 50^\circ$.

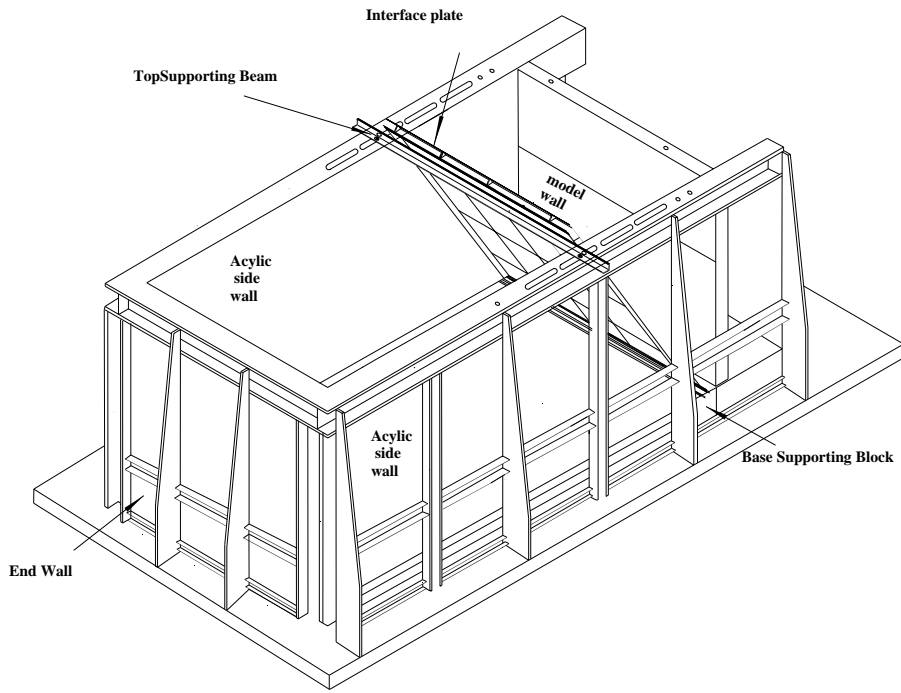
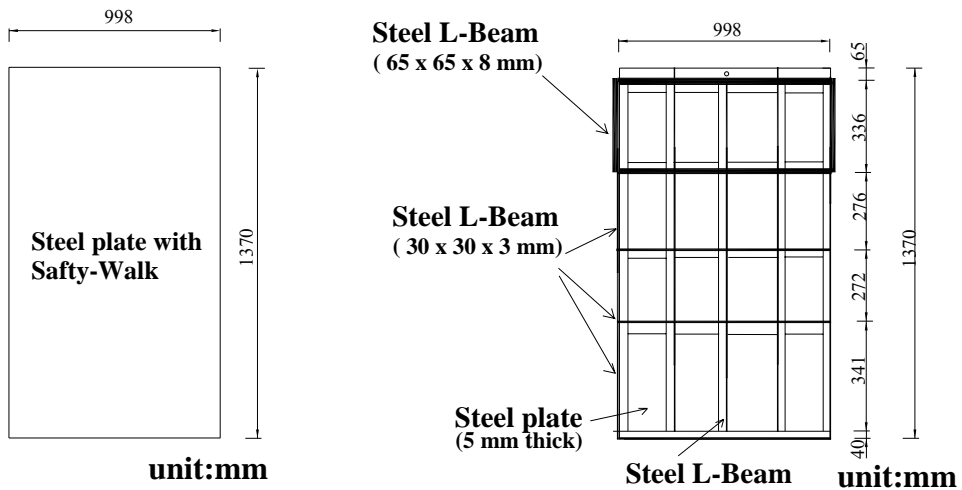
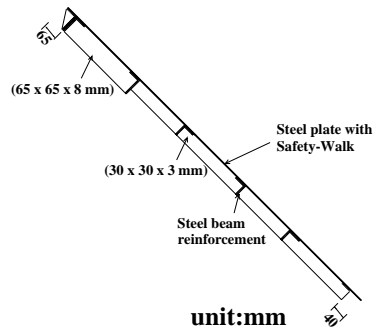


Fig. 4.1. NCTU model retaining wall with inclined interface plate



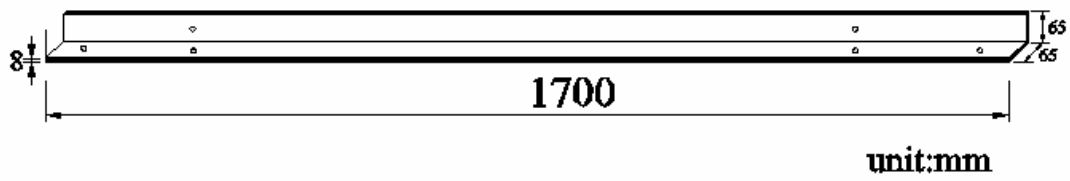
(a) Front-view

(b) Back-view



(c) Side-view

Fig. 4.2. Steel interface plate

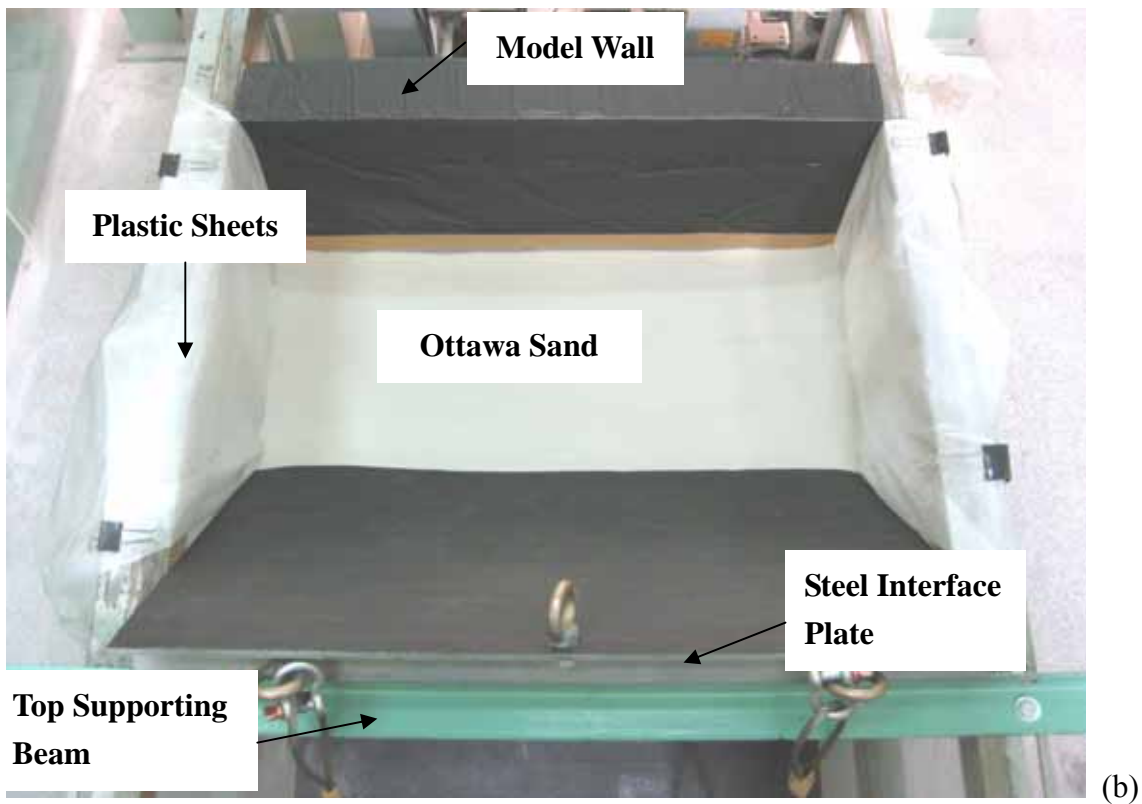


(a)



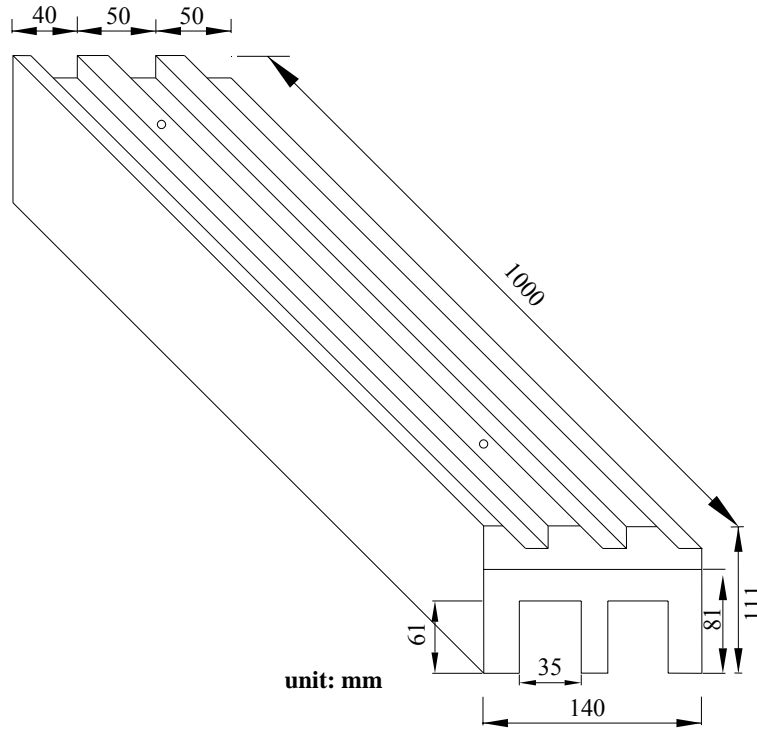
(b)

Fig. 4.3. Top supporting beam



(b)

Fig. 4.4. Model retaining wall and steel interface plate



(a)



(b)

Fig. 4.5. Base supporting block

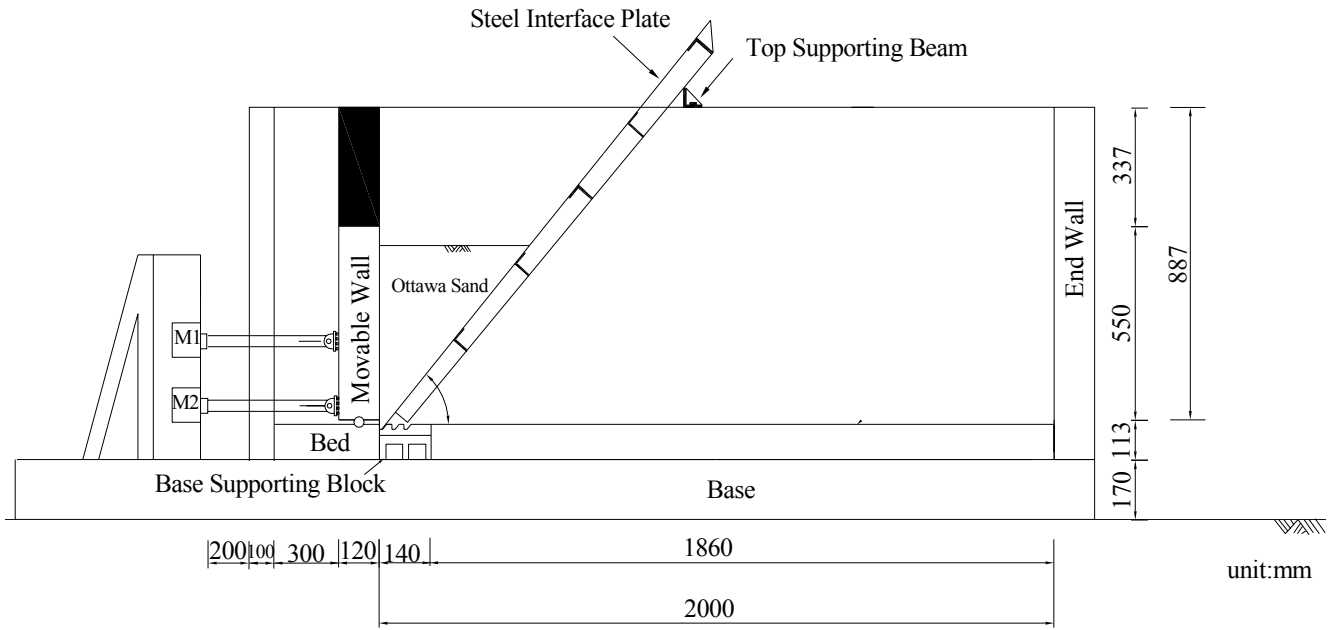


Fig. 4.6. NCTU model retaining wall with interface plate supports

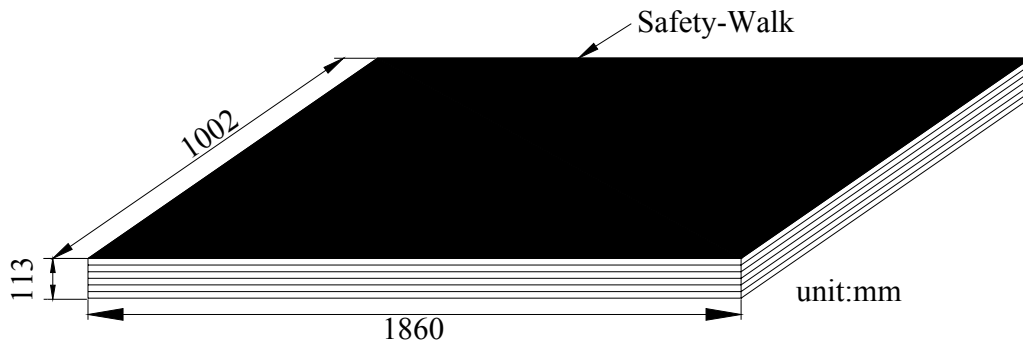


Fig. 4.7. Base boards

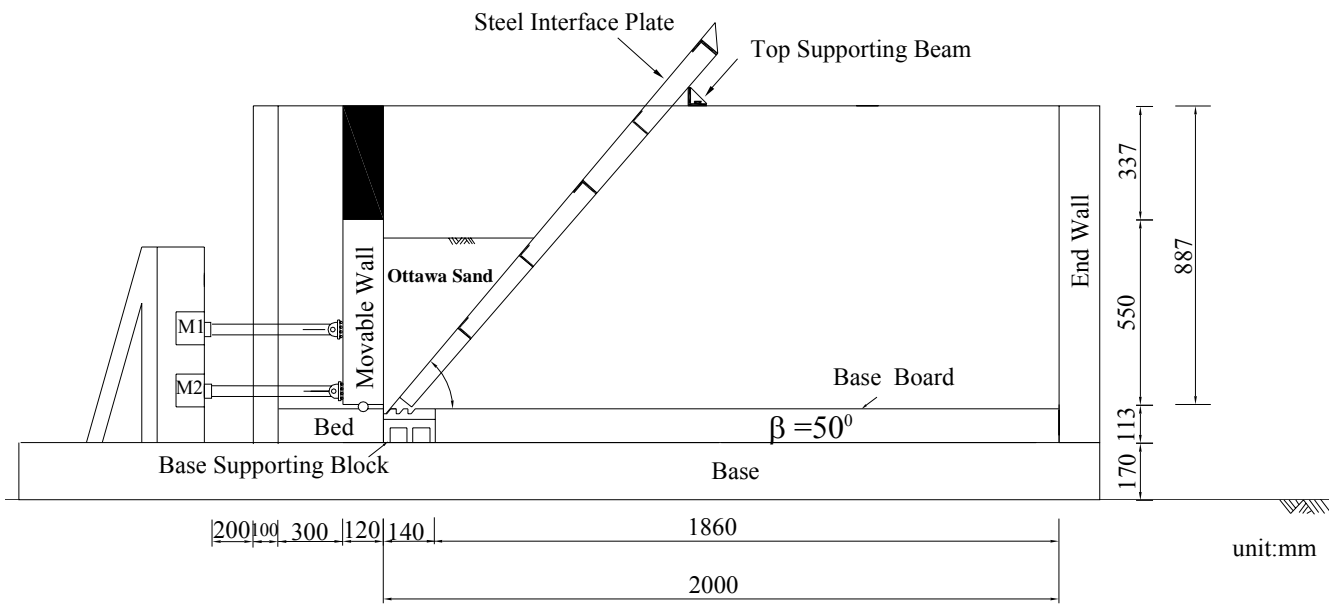


Fig. 4.8. Model wall test with interface inclination $\beta = 50^\circ$

5. BACKFILL AND INTERFACE CHARACTERISTICS

5.1 Backfill Properties

Air-dry Ottawa silica sand (ASTM C-778) was used as backfill. For the air-pluviated backfill, an empirical relationship between soil unit weight γ and ϕ angle was formulated as follows:

$$\phi = 6.43 \gamma - 68.99 \quad (5.1)$$

where ϕ = angle of internal friction of soil (degree); γ = unit weight of soil (kN/m³); Eq. 5.1 was applicable for $\gamma = 15.45 \sim 17.4$ kN/m³ only.

5.2 Side Wall Friction

To reduce the friction between sidewall and backfill, a lubrication fabricated layer with plastic sheets was furnished for all model wall experiments. For the plastic sheet arrangement (1 thick + 2 thin sheetings) used in this study, the measured friction angle with this method was about 7.5°.

5.3 Model Wall Friction

To evaluate the wall friction angle δ_w between the backfill and model wall, special direct shear tests had been conducted. A 88 mm × 88 mm × 25 mm smooth steel plate, made of the same material as the model wall, was used as the lower shear box. Ottawa sand was placed into the upper shear box and vertical load was applied on the soil specimen. For air-pluviation Ottawa sand, Lee (1998) suggested the following relationship:

$$\delta_w = 3.41 \gamma - 43.69 \quad (5.2)$$

Where δ_w = wall friction angle (degree), and γ = unit weight of backfill (kN/m³), Eq. 5.2 was applicable for $\gamma = 15.5 \sim 17.5$ kN/m³ only.

5.4 Inclined Interface Friction

To evaluate the interface friction between the interface plate and the backfill, special direct shear tests were conducted. A 80 mm × 80 mm × 15 mm steel plate was covered with a layer of anti-slip material “Safety-Walk” to simulate the surface the inclined rock. For air-pluviation Ottawa sand, Wang (2005) suggested the following empirical relationship:

$$\delta_i = 2.7\gamma - 21.39 \quad (5.3)$$

Where δ_i = interface-plate friction angle (degree), and γ = unit weight of soil (kN/m^3). Eq. 5.3 was applicable for $\gamma = 15.1 \sim 16.36 \text{ kN/m}^3$ only.

5.5 Control of Soil Density

To achieve a uniform soil density in the backfill, dry Ottawa sand was deposited by air-pluviation method into the soil bin. As indicated in Fig. 5.1, the soil hopper let the soil particles pass through a calibrated slot opening at its lower end. In this study, the drop height of 1.0 m and the slot opening of 15 mm were selected to achieve the loose backfill with a relative density of 35%.

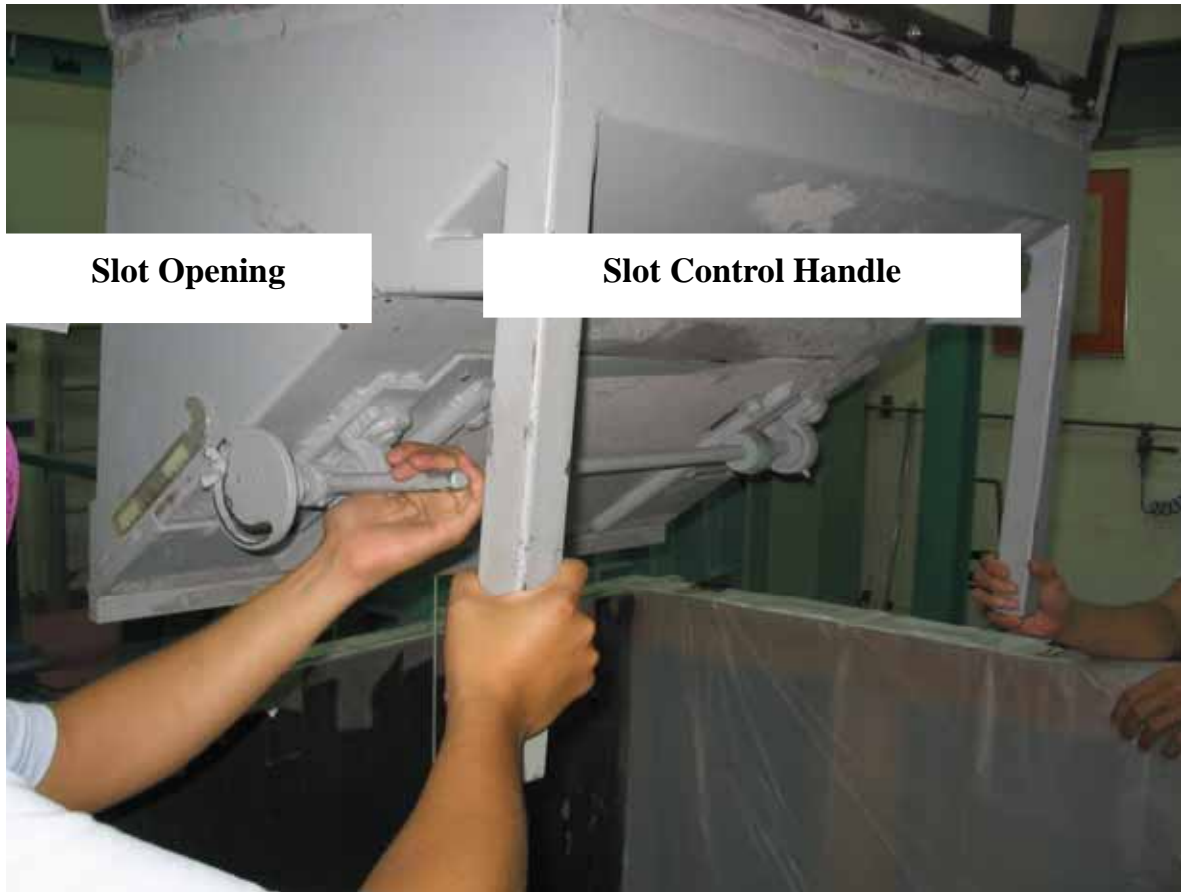


Fig. 5.1. Soil hopper

6. EXPERIMENTAL RESULTS

This chapter reports the experimental results regarding effects of an adjacent inclined rock face on the active earth pressure against a retaining wall. The loose ($D_r = 35\%$) Ottawa sand with the unit weight $\gamma = 15.6 \text{ kN/m}^3$ was prepared as the backfill material. Based on direct shear tests, the corresponding internal friction angle ϕ is 31.3° . The γ and ϕ values were used to calculate the earth pressures based on the Jaky and Coulomb theories.

6.1 Distribution of Earth Pressure

The distributions of active earth pressure at the interface inclination angle $\beta = 0^\circ, 50^\circ, 60^\circ, 70^\circ$ and 80° were shown in Fig. 6.1. In the figure, the active earth pressure decreases with increasing β angle. It would be reasonable to expect that the magnitude of active soil thrust to decrease with increasing β angle. For the β angle greater than 50° , the shape of the active pressure distribution implied that the point of application of the active soil thrust would not be significantly affected by the rock face inclination angle β .

6.2 Magnitude of Soil Thrust

The variation of active earth pressure coefficient $K_{a,h}$ as a function of interface inclination angle β was shown in Fig. 6.2. For comparison purposes, the analytical results reported by Fan and Chen (2006) were also plotted in Fig. 6.2. Without the interface plate ($\beta = 0^\circ$), the coefficient $K_{a,h}$ values was in fairly good agreement with Coulomb's prediction. However, with the intrusion of the rock face into the active soil wedge, the coefficient $K_{a,h}$ decreased with increasing rock face inclination angle β . Although the tend was the same, the experimental $K_{a,h}$ was much lower than the numerically obtained $K_{a,h}$ values.

6.3 Point of Application of Soil Thrust

Fig. 6.2 showed the variation of the point of application of active soil thrust with the β angle. For the $\beta = 0^\circ$, no rock face was near the retaining wall, the $(h/H)_a$ value was located at about $0.33H$ above the base of the wall. As the interface angle β increased, the earth pressure measured near the base of the wall decreased. This change of earth pressure distribution caused the active total thrust to move to a slightly higher location as shown in Fig. 6.3. For $\beta = 80^\circ$, the point of application of the active soil thrust was located at $0.425H$ above the base of the wall..

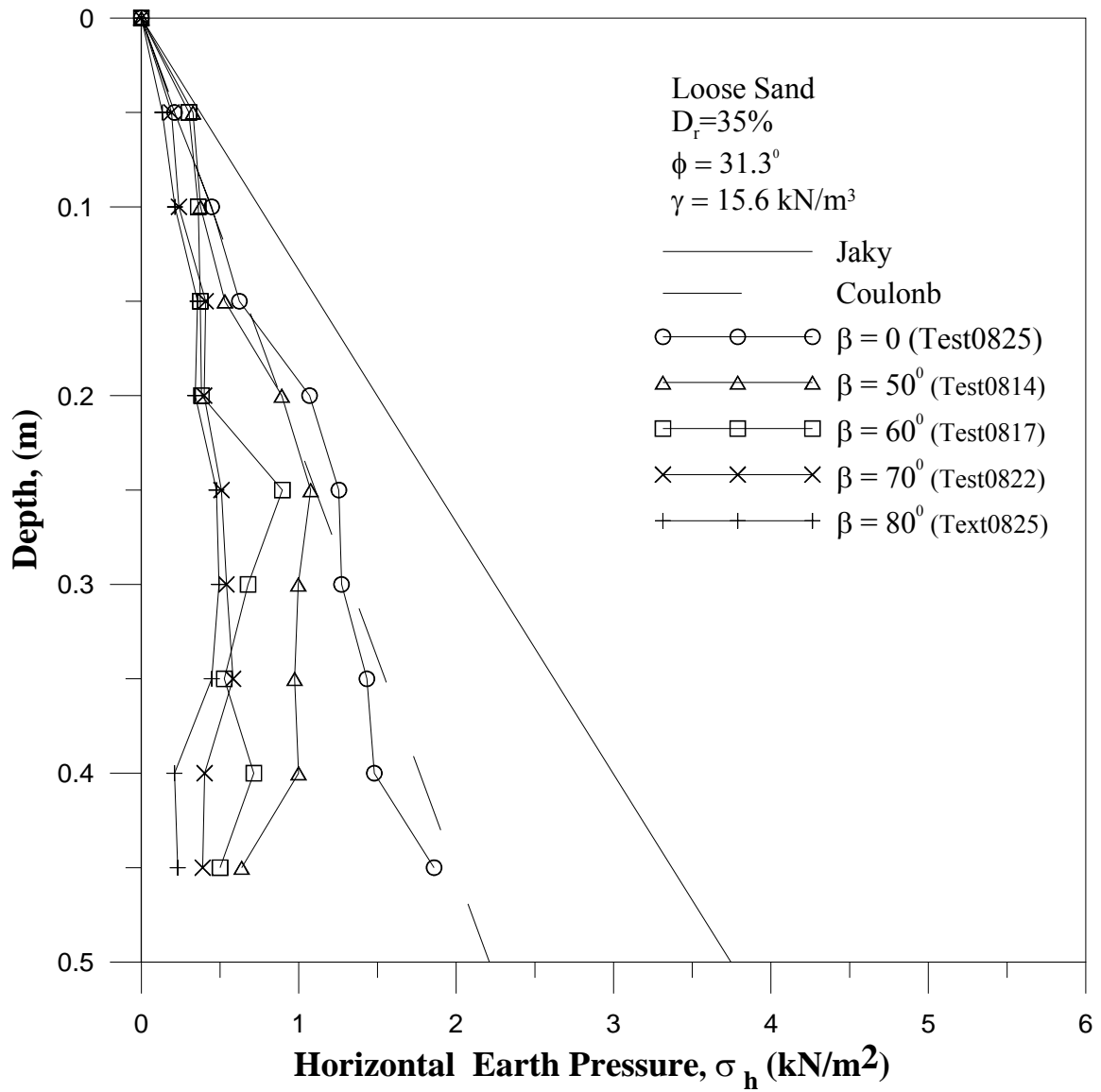


Fig. 6.1 Distribution of active earth pressure at different interface inclination angle β

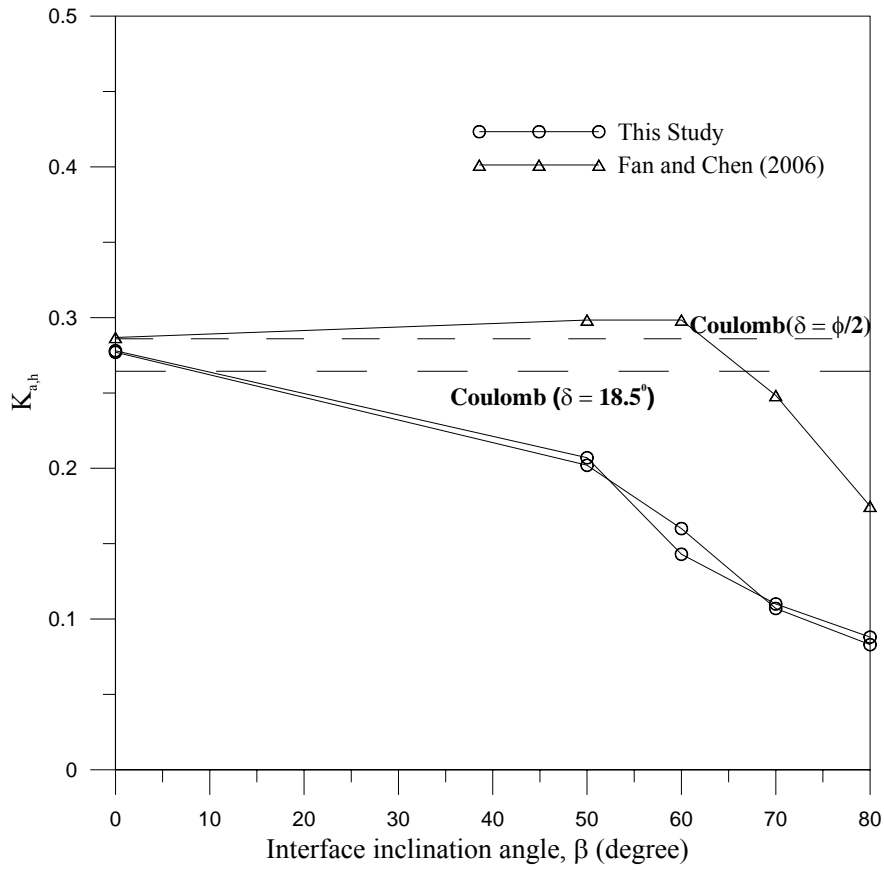


Fig. 6.2. Active earth pressure coefficient $K_{a,h}$ versus interface inclination angle β

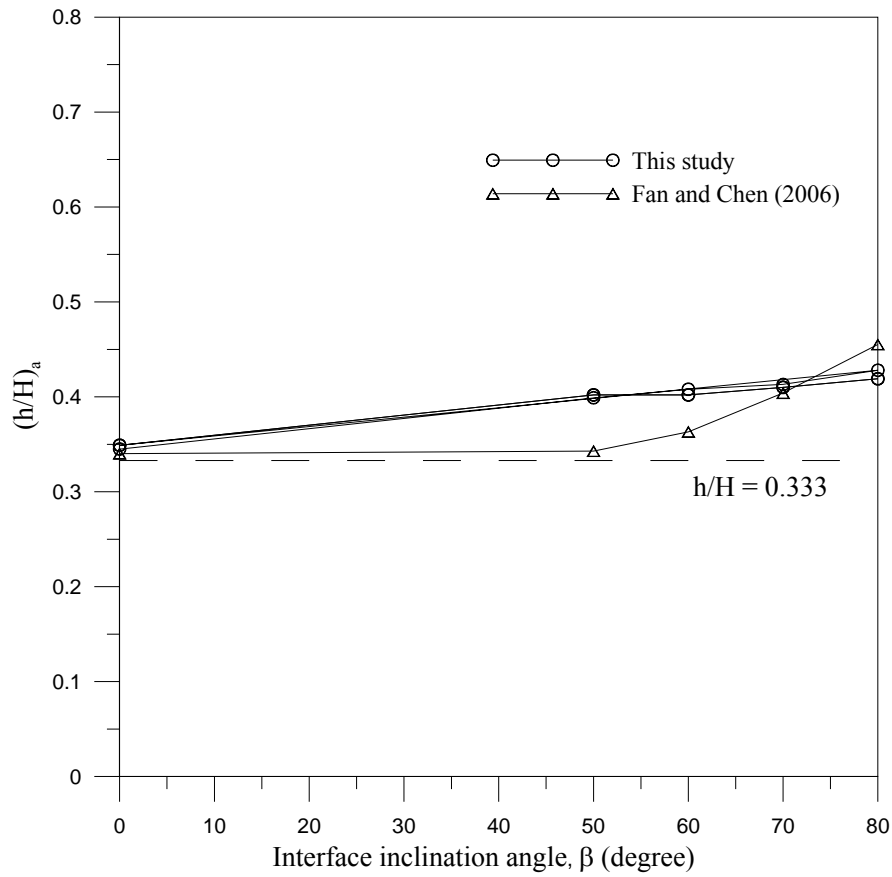


Fig. 6.3. Point of application of active soil thrust versus interface inclination angle β

7. CONCLUSIONS

In this study, the effects of a nearby inclined rock face on the active earth against a rigid retaining wall were investigated. Based on the test results, the following conclusions can be drawn.

1. Without the Stiff interface ($\beta = 0^\circ$), the active earth pressure coefficient $K_{a,h}$ was in good agreement with Coulomb's equation. The point of application h/H of the active soil thrust was located at about $0.33H$ above the base of the wall.
2. For the interface inclination angle $\beta = 50^\circ, 60^\circ, 70^\circ$ and 80° , the distributions of active earth pressure were not linear with depth. On the lower part of the model wall the measured horizontal pressure was lower than Coulomb's solution.
3. For $\beta = 50^\circ \sim 80^\circ$, the active earth pressure coefficient $K_{a,h}$ decreased with increasing β angle. The point of application of the active total thrust moved to a location slight higher than $h/H = 0.333$.
4. For $\beta = 50^\circ \sim 80^\circ$, the nearby inclined rock face would actually increase the FS against sliding of the wall. The evaluation of FS against sliding with the Coulomb theory would be on the safe side.
5. For $\beta = 50^\circ \sim 80^\circ$, the intrusion of an inclined rock face into the active soil wedge would increase the FS against overturning of the wall. The evaluation of FS against overturning with the Coulomb theory would also be on the safe side.

8. REFERENCES

1. Bakeer, R. M., and Bhatia, S. K., (1989), "Earth Pressure Behind a Gravity Retaining Wall," *International Journal for numerical and Analytical Methods in Geomechanics*, Vol. 13, pp. 665-973.
2. Bros, B. (1972). "The influence of model retaining wall displacements on active and passive earth pressures in sand." *Proc., 5th European Conf. on Soil Mechanics*, Madrid, 1, 241-249.
3. Chen, T. J., (2003), "Earth Pressure Due to Vibratory Compaction", *Doctor of Philosophy Dissertation*, National Chiao Tung University, Hsinchu, Taiwan.
4. Fan, C. C., and Chen K. H, (2006), "Earth Pressure of Retaining Wall near Rock Face," *Master of Engineering Thesis*, Department of Construction Engineering, National Kaohsiung First University of Science and Technology, Taiwan.
5. Fang, Y. S., and Ishibashi, I., (1986), "Static Earth Pressures with Various Wall Movements," *Journal of Geotechnical Engineering*, ASCE, Vol. 112, No. 3, Mar., pp. 317-333.
6. Fang, Y. S., Cheng F. P., Cheng, R. T., and Fan, C. C., (1993), "Earth Pressure under General Wall Movements," *Geotechnical Engineering*, SEAGS, Vol. 24, No. 2, December., pp. 113-131.
7. Fang, Y. S., Chen, T. J., and Wu, B. F. (1994). "Passive earth pressures with various wall movements." *Journal of Geotechnical Engineering*, ASCE, 120(8), 1307-1323.
8. Fang, Y. S., Chen, J. M., and Chen, C. Y., (1997), "Earth Pressures with Sloping Backfill,"

Journal of Geotechnical and Geoenvironmental Engineering, ASCE, Vol. 123, No. 3, March, pp. 250-259.

9. Fang, Y. S., Chen, T. J., Holtz, R. D., and Lee, W. F., (2004), "Reduction of Boundary Friction in Model Tests", *Geotechnical Testing Journal*, ASTM, Vol. 27, No. 1, pp. 1-10.
10. Frydman, S., and Keissar, I., (1987), "Earth Pressure on Retaining Walls near Rock Faces." *Journal of Geotechnical Engineering*, Vol. 113, June, pp. 586-599.
11. Mackey, R. D., and Kirk, D. P., (1967), "At Rest, Active and Passive Earth Pressures," *Proceedings*, South East Asian Conference on Soil Mechanics and Foundation Engineering, Bangkok, pp. 187-199.
12. Matsuzawa, H., and Hazarika, H., (1996), "Analyses of Active Earth Pressure Against Rigid Retaining Wall Subjected to Different Modes of Movement," *Soils and Foundations*, Japanese Geotechnical Society, Vol. 36, No. 3, pp. 51-65.
13. Sherif, M. A., Ishibashi, I., and Lee, C. D., (1982), "Earth Pressure Against Rigid Retaining Walls," *Journal of Geotechnical Engineering*, ASCE, Vol.108, No.GT5, May, pp. 679-695.
14. Terzaghi, K., (1934), "Large Retaining-Wall Tests," *Engineering News-Record*, pp. 136-140.

9. 計劃成果自評

本研究利用國立交通大學模型擋土牆設備來探討堅硬以不同界面傾角 β 侵入回填土對擋土牆主動土壓力影響。為了模擬堅硬的土層界面，本研究設計並建造一片鋼製傾斜界面板，及其支撐系統。本研究以氣乾渥太華砂作為回填土，回填土高 0.5 m，量測於鬆砂($D_r = 35\%$)狀態下作用於剛性擋土牆的側向土壓力。本研究共執行五種堅硬界面傾角 $\beta = 0^\circ$ 、 50° 、 60° 、 70° 與 80° 五種實驗。依據擋土牆砂實驗結果，本研究獲得以下幾項結論。(1) 當岩石界面傾角 $\beta = 0^\circ$ 時，其主動土壓力係數 $K_{a,h}$ 與 Coulomb 解相吻合，其主動合力約作用於距擋土牆底部 $0.33H$ 處。(2) 在岩石界面傾角 45° 、 60° 、 70° 與 80° 狀況下，主動土壓力隨深度的增加而呈非線性分布，所獲得的主動土壓力低於 Coulomb 解，主動土壓力隨界面傾角的增加而減少。(3) 當界面傾角 β 為 50° 至 80° ，主動土壓力係數 $K_{a,h}$ 數隨岩石界面傾角的增加而逐漸減小。其合力作用點的位置會稍高於理論值 $0.333H$ 。(4) 當傾斜岩石面入侵主動土楔時，造成擋土牆抗滑動之安全係數增加，因此根據 Coulomb 理論所求解之安全係數會偏向安全。(5) 當傾斜岩石面入侵土楔時，由於主動土壓力降低，使得擋土牆抗傾覆之安全係數增加，所以依據 Coulomb 理論所求得之抗傾覆安全係數會趨於安全。本研究內容與計劃書完全相符。

本研究獲得數項創新且具有實用性的之研究成果，充分達成預期之目標，將於近期內投稿至國際知名期刊。參與研究的碩士班研究生藉此機會，學習大型基礎模型實驗及資料擷取系統之操作，習得嚴謹的實驗方法及獲得獨立解決問題的能力，獲益良多。

可供推廣之研發成果資料表

可申請專利

可技術移轉

日期：97年7月31日

國科會補助計畫	<p>計畫名稱：堅硬土層侵入回填土對擋土牆靜止主動及被動土壓力之影響(3/3)</p> <p>計畫主持人：方永壽 教授</p> <p>計畫參與人員：鄭詠誠、吳俊德 碩士班研究生</p> <p>計畫編號： NSC 96-2221-E-009-004-</p> <p>學門領域： 土木水利工程</p>
技術/創作名稱	
發明人/創作人	
技術說明	<p>中文： 本研究利用國立交通大學模型擋土牆設備來探討堅硬以不同界面傾角β侵入回填土對擋土牆主動土壓力影響。堅硬界面傾角β分別為 0°、50°、60°、70° 與 80°，依擋土牆砂實驗結果，本研究獲得以下幾項結論。(1)當岩石界面傾角$\beta=0^\circ$時，其主動土壓力係數 $K_{a,h}$ 與 Coulomb 解吻合，其主動合力約作用於距擋土牆底部 $0.33H$ 處。(2) 在岩石界面傾角 50°、60°、70° 與 80° 狀況下，主動土壓力隨深度的增加而呈非線性分布，所獲得的主動土壓力低於 Coulomb 解，主動土壓力係數 $K_{a,h}$ 隨岩石界面傾角β的增加而逐漸減小，主動土壓合力作用點的位置會稍高於理論值 $0.333H$。(3)當傾斜岩石面入侵主動土楔時，造成擋土牆抗滑動及抗傾覆之安全係數增加，因此根據 Coulomb 理論所求解之安全係數會偏向安全。</p> <p>英文： This report studied the active earth pressure on retaining walls with the intrusion of an inclined rock face into the backfill. Ottawa silica sand was used as the backfill material. Base on the test results, the following conclusions can be drawn. (1) Without the Stiff interface ($\beta = 0^\circ$), the active earth pressure coefficient $K_{a,h}$ was in good agreement with Coulomb's equation. (2) For the interface inclination angle $\beta = 50^\circ, 60^\circ, 70^\circ$ and 80°, the distributions of active earth pressure were not linear with depth. The active earth pressure coefficient $K_{a,h}$ decreased with increasing interface inclination angle. The point of application of the active soil thrust moved a location slightly higher than $h/H = 0.333$. (3) For $\beta = 50^\circ \sim 80^\circ$, the nearby inclined rock face would actually increase the FS against sliding and overturning of the wall. The evaluation of FS against sliding and overturning with Coulomb's theory would be on the safe side.</p>
推廣及運用的價值	<p>本研究屬於基礎學術性研究，三年計畫完成，所獲研究結果將有助於世界各國擋土結構物設計的參考。</p>

1.每項研發成果請填寫一式二份，一份隨成果報告送繳本會，一份送 貴單位研發成果推廣單位（如技術移轉中心）。

2.本項研發成果若尚未申請專利，請勿揭露可申請專利之主要內容。

3.本表若不敷使用，請自行影印使用。